FURTHER OBSERVATION OF DIMUON PRODUCTION BY NEUTRINOS*

A. Benvenuti, D. Cline, W. T. Ford, R. Imlay, T. Y. Ling, A. K. Mann, R. Orr, D. D. Reeder, C. Rubbia, R. Stefanski, L. Sulak and P. Wanderer

Department of Physics
Harvard University
Cambridge, Massachusetts 02138

Department of Physics
University of Pennsylvania
Philadelphia, Pennsylvania 19174

Department of Physics
University of Wisconsin
Madison, Wisconsin 53706

Fermi National Accelerator Laboratory
P. O. Box 500
Batavia, Illinois 60510

Abstract

Using a quadrupole focussed neutrino beam, 61 events with two muons in the final state have been observed in the HPWF detector at Fermilab. These include 7 $\mu^-\mu^-$ events. A comparison of the event rate in two targets of different hadron absorption length indicates that attributing the events to π or K leptonic decay is ruled out by 4.0 standard deviations. No trimuon events were observed which, combined with lepton conservation, indicates a missing neutral lepton is present in most of the events.

We have reported previously evidence for dimuon production by neutrinos.[1,2] The experimental absence of trimuon events and the predominance of opposite electric charges for the observed events was used to infer from lepton conservation that these events have a missing neutrino.[2] The interpretation of these events requires new particle production. In order to confirm the existence of dimuon events a new experiment was carried out and the results are reported here.[3]

The HPWF calorimeter-magnetic spectrometer[4] was exposed to a very high energy neutrino beam obtained from quadrupole focussing of the parent hadrons. The quadrupole triplet was set to focus 200 GeV charged hadrons and the primary proton energy was 380 GeV. This beam is predominately composed of neutrino with a small admixture of antineutrinos ($\sim$1/7). A beam spill of $\sim$1 ms was used to minimize accidental coincidences. Events were detected in two separate targets, the liquid scintillation calorimeter and a large block of iron adjacent to the calorimeter (Hadron Filter). The trigger requirement for all events was either a single muon that penetrated the entire magnetic spectrometer or an energy deposition in the calorimeter.

A total of 114 dimuon candidates were observed and the events were distributed as 58 and 56 for the iron and liquid targets, respectively. In about 30% of the events one of the muons failed reconstruction because of chamber topology. The final number of reconstructed events from each target was 41 and 36 respectively. No events with three muons were observed.

The momentum and angle of each muon was measured and extrapolated back into the appropriate target. The distance (Δ) between the extrapolated rays at the interaction point, determined by appropriate counters, is shown in Fig. 1a. Events with $\Delta < 50$ cm were accepted in the sample provided

they passed additional requirements such as correct timing and correct position of the muon tracks in a 16 element hodoscope located in the magnetic spectrometer. The long spill of the neutrino beam and the time and space resolution of the detector reduce the probability of an accidental space-time coincidence of two independent muons to a negligible level. Figure 1b shows the resulting z (along the beam direction) distribution for the events. After applying a fiducial volume cut to the data there remained 27 and 34 events originating in the calorimeter and hadron filter, respectively.

The events were corrected for geometrical loss, i.e., the requirement that both tracks from an event pass through at least two spark chambers, using a Monte Carlo calculation. Each event was assigned a geometrical detection efficiency and a corresponding weight.

To calculate the event rate for $\mu^+\mu^-$ production a sample of 18 $\mu^+\mu^-$ events were selected in a further restricted fiducial volume in which 6200 single muon events were also recorded. Applying the geometrical and estimated reconstruction efficiency to this sample gave for a $\mu^+\mu^-$ to single muon ratio $(0.8 \pm 0.3) \times 10^{-2}$ where the error includes statistical and estimated systematic uncertainties.

In order to test the sample of $\mu^+\mu^-$ dimuons for the presence of a background which might arise from neutrino-induced single muon events followed by the decay of a pion or kaon into a muon and neutrino, a comparison between the event rates for the calorimeter sample and the hadron filter sample was carried out. This comparison makes use of the different absorption lengths of the liquid scintillator and the hadron filter. The fraction of events originating from pion or kaon decays is defined as α, which is determined in turn from the dependence of the event rate on absorption length.

Table 1 lists the corrected rates for the calorimeter and hadron filter samples. To eliminate trigger bias we require here that at least one muon traverses the entire spectrometer. Note that the mass of the two targets are approximately the same. Note also that the rate for calorimeter and hadron filter events is the same when a restrictive $p_\mu > 10$ GeV momentum cut is required for individual muons. While (π, K) background contamination is expected to increase rapidly with the decreasing momentum, there is no observed difference between the ratio of rates in the different targets for the lower and higher muon momentum samples. In Fig. 2a is plotted the event rate for the two different absorption lengths.[5] The significant rate at the extrapolated zero absorption length indicates the existence of muon production arising from sources that are necessarily much shorter lived than π or K mesons. A maximum likelihood analysis for α, incorporating the different absorption lengths and the detection efficiencies for events in the two targets, is presented in Fig. 2b. The best solution gives $\alpha = 0$ and is four standard deviations away from the solution $\alpha = 1$.

While the sample of $\mu^-\mu^-$ events is too small to obtain a statistically meaningful comparison we note that if all the events were due to (π^-, K^-) decay, from the observed 4 events in the hadron filter and the estimated ratio of absorption lengths of 3.54, the number of events expected in the calorimeter is 14 as compared to the one event observed. Additionally, if both μ^- are required to have momenta greater than 10 GeV, only the four events in the hadron filter remain. It is thus unlikely that the $\mu^-\mu^-$ events can be explained as (π^-, K^-) decay background. In Table 2 are listed the parameters for the $\mu^-\mu^-$ events. From the corrected number of events recorded in Table 1 the ratio of rates for $\mu^-\mu^-$ to $\mu^+\mu^-$ production is found to be $0.1 \pm .05$.

Note that three $\mu^+\mu^+$ events were also observed as listed in Table 2.

The projected transverse momentum P_{t2} with respect to the plane formed by the incident neutrino and the first muon (p_1) is given by[2]

$$P_{t2} = \frac{\vec{P}_2 \cdot (\vec{P}_\nu \times \vec{P}_1)}{|\vec{P}_\nu \times \vec{P}_1|}$$

The plane must also contain the momentum vector of the recoiling hadronic jet, and therefore P_t is the projected transverse momentum with respect to the hadronic jet. If the muon arises from pion decay, P_t is very closely the projected transverse momentum of the pion and the resulting distribution is expected to fall exponentially with P_t. If the muon along with a missing neutrino arises from the decay of a massive new hadron, then the P_t distribution is characteristic of the mass and decay final states of the new particle. Figure 3 shows the P_t distributions for the $\mu^+\mu^-$ events (Fig. 3a, 3b, 3c) and $\mu^-\mu^-$ events (Figs. 3d, 3e, 3f) for increasing muon momentum cuts. In the case of the $\mu^-\mu^+$ events P_t^+ has been plotted whereas for the $\mu^-\mu^-$ evnts the P_t corresponding to the lowest momentum muon (i.e. P_{t2} with $P_1 > P_2$). The P_t distribution for the $\mu^-\mu^+$ events (Figs. 3a, 3b, 3c) are inconsistent with an exponential fall off that is characteristic of (π, K) production as observed in neutrino collisions.[6] The trend of the P_t distribution for the $\mu^-\mu^-$ events (Figs. 3d, 3e) is also not characteristic of (π, K) production and decay and provides additional support for the existence of $\mu^-\mu^-$ production that is not caused by (π, K) decay. We note that the P_t distributions for both $\mu^-\mu^+$ and $\mu^-\mu^-$ events appear to cut off at roughly $P_t \simeq 1$ GeV/c.

A further related characteristic of the dimuon events is the distribution of the azimuthal angle between the muon momentum vectors projected on

a plane normal to the neutrino direction. This correlation is shown in Fig. 4a for both the $\mu^-\mu^+$ and $\mu^-\mu^-$ events. For the $\mu^-\mu^+$ events there is a tendency for two muons to emerge on opposite sides of the neutrino beam and there are an appreciable number of events with both muons on the same side of the neutrino beam direction. The $\mu^-\mu^-$ events are nearly uniformly distributed in angle.

The neutrino energy dependence of dimuon production is of interest in establishing the origin of the phenomena. In a previous experiment the observed fraction of dimuons relative to single muon production was found to be $(0.9 \pm 0.3) \times 10^{-2}$ where the error is statistical only.[2] The mean visible energy for these events was 55 GeV. Within error the corresponding ratio has not changed in the present experiment where the mean neutrino energy is roughly 100 GeV. Since the total neutrino cross section is found to rise linearly in this energy region it appears that the dimuon cross section also rises with neutrino energy.[4] Additional support for this conclusion is obtained from the μ^- momentum spectrum shown in Fig. 4b. Using a flat y distribution, the calculated neutrino spectrum for the quadrupole triplet beam and a linearly rising cross section allows a prediction for the μ momentum spectrum which is also shown in Fig. 4b.[7] The rough agreement of the prediction and the data in Fig. 4b is consistent with the assumption of a linear rising dimuon cross section. Note that if dimuon events with $p_{\mu^+} > p_{\mu^-}$, which may be examples of antineutrino events, are removed from the sample, the resulting μ^- spectrum would be distorted in the low momentum region compared to the predicted distribution. This distortion might be caused by a threshold in the dimuon cross section at low neutrino energy.

In summary, the work reported here has established a dimuon signal

that does not arise from the decay of pions or kaons produced in neutrino collisions. This conclusion is model independent and only depends on the hadronic absorption characteristics of pions and kaons.

The first examples of $\mu^-\mu^-$ events have been observed and are also shown to be unlikely to arise from (π, K) decay. The $\mu^-\mu^+$ dimuon production follows a rising cross section with neutrino energy; and a threshold behavior with neutrino energy is not ruled out. Finally the projected transverse momentum spectrum is cut off at $\sim$1 GeV/c suggesting that a mass near or greater than 2 GeV/c^2 characterizes the dimuon events.

It is a pleasure to acknowledge the aid and encouragement of the Fermilab staff.

References

*Work supported in part by the U. S. Energy Research and Development Administration.

1. B. Aubert et al., "Experimental Observation of $\mu^+\mu^-$ Pairs Produced by Very High Energy Neutrinos", in Proceedings of the Seventeenth International Conference on High Energy Physics, London, 1974 and in Neutrinos - 1974, AIP Conference Proceedings No. 22, edited by C. Baltay (American Institute of Physics, New York, 1974), p. 201.
2. A. Benvenuti, et al., Phys. Rev. Letters 34, 419 (1975), ibid. 34, 597 (1975).
3. Additional evidence for the production of dimuon events has recently been given by B. Barish et al., Proceedings of the Paris Neutrino Conference, p. 131 (1975).
4. A. Benvenuti, et al., Phys. Rev. Letters 32, 125 (1974).

5. The absorption length of the liquid has been directly measured by us to be 118 ± 5 cm using an incident π beam. The absorption length for the hadron filter was obtained from the known absorption length of pions in iron and a calculation that took into account the air gaps. S. P. Denisov, Nucl. Phys. B61, 62 (1973).

6. Private communication, F. Nezrick.

7. A. Benvenuti, et al., A Simple Focussed Neutrino Beam, Proceedings of the Paris Neutrino Conference, p. 397 (1975).

Figure Captions

Fig. 1a The distribution in the distance between the extrapolated muon tracks at the Z position where the interaction occurred.

Fig. 1b Distribution of the dimuon event interaction vertices along the Z direction.

Fig. 2a The number of events recorded per gm/cm^2 of target for the different absorption lengths of the two targets. The line is an extrapolation to zero absorption length.

Fig. 2b Results of the likelihood analysis of the fraction, α of events that arise from π or K decays.

Fig. 3a The distribution of the μ^+ momentum component transverse to the μ^- - neutrino plane (P_t) for all μ^+ momenta. (b) Same as (a) but requiring $p_{\mu^+} \geq 10$ GeV/c. (c) Same as (b) except $p_{\mu^+} \geq 20$ GeV/c is required. (d) The P_t distribution for the $\mu^-\mu^-$ events, for the lowest momentum μ^-. (e) Same as (d) except the lowest momentum μ^- is required to have $p_{\mu^-} \geq 10$ GeV/c. (f) Same as (d) except for the requirement that the lowest momentum μ^- have $p_{\mu^-} \geq$ 20 GeV/c.

Fig. 4a The difference in azimuthal angles for the μ^+ and μ^- muons. The neutrino beam direction heads into the paper and μ_1, μ_2 are the muon momenta projected on the (x, y) plane. Also shown is the same difference plotted for the $\mu^-\mu^-$ events.

Fig. 4b The μ^- momentum spectrum compared with the expected spectrum obtained for the assumption of a linearly rising total cross section and a flat y distribution. The cross hatched data refers to possible antineutrino events for which $p_{\mu^+} > p_{\mu^-}$.

Tables

Table 1 The number of events observed in the liquid scintillator and hadron filter targets. Both corrected and uncorrected numbers of events are reported.

Table 2 Parameters of the $\mu^-\mu^-$ and $\mu^+\mu^+$ events. $P_{1,2}$ refer to the muon momenta and E_H to the hadronic energy. θ_{12} is the opening angle between the two muons. $v_{1,2}$ is defined as $(2E_\mu \sin^2\theta_\mu/2)/M_p$ where θ_μ is the muon angle with respect to the neutrino beam direction. The measured values are uncertain to approximately ±15% in most cases.

Table 1

Rate in Liquid Scintillator vs. Hadron Filter

Target	No. of $\mu^-\mu^+$		No. of $\mu^-\mu^-$		Target Mass gm/cm^2	Selection Criteria
	Raw	Corr.	Raw	Corr.		
Cal	19	29.1 ± 8.2	1	1.8	576	Fiducial Cut and Identical Trigger Requirements
Hadron Filter	23	28.7 ± 8.3	4	4.3	590	
Cal	11	15.2 ± 4.6	0	0	576	Above Requirements and $P_{\mu 1} > 10$ GeV $P_{\mu 2} > 10$ GeV
Hadron Filter	12	13.8 ± 4.0	4	4.3	590	

Table 2

Parameters of the $\mu^-\mu^-$ and $\mu^+\mu^+$ Events

Event Number	Event Weight	Target	E_H (GeV)	P_1 (GeV/c)	P_2 (GeV/c)	θ_{12} (mr)	v_1	v_2	P_{t1} (GeV/c)	P_{t2} (GeV/c)
573874	.96	Filter		53.3	11.5	111	.07	.024	.58	.16
575921	.97	Filter		30.6	14.0	67	.04	.09	.6	.6
585090	.98	Filter		57.9	38.8	89	.095	.024	.34	.14
603533	.98	Filter		25.2	12.8	81	.002	.06	.09	.36
609761	.51	Calorimeter	123	51.7	6.1	65	.09	.03	1.9	.38
574313	.66	Filter		14.1	5.5	300	.76	.14	4.0	1.1
614121	.06	Calorimeter	22	19.9	4.2	295	.42	.03	2.7	.33
561828**	.58	Calorimeter	22	8.8	4.8	68	.15	.04	.36	.13
611084**	.96	Filter		17.5	9.1	255	.2	.06	.17	.07
622417**	.66	Filter		28.5	2.4	125	.1	.003	.05	.00

**$\mu^+\mu^+$ Events

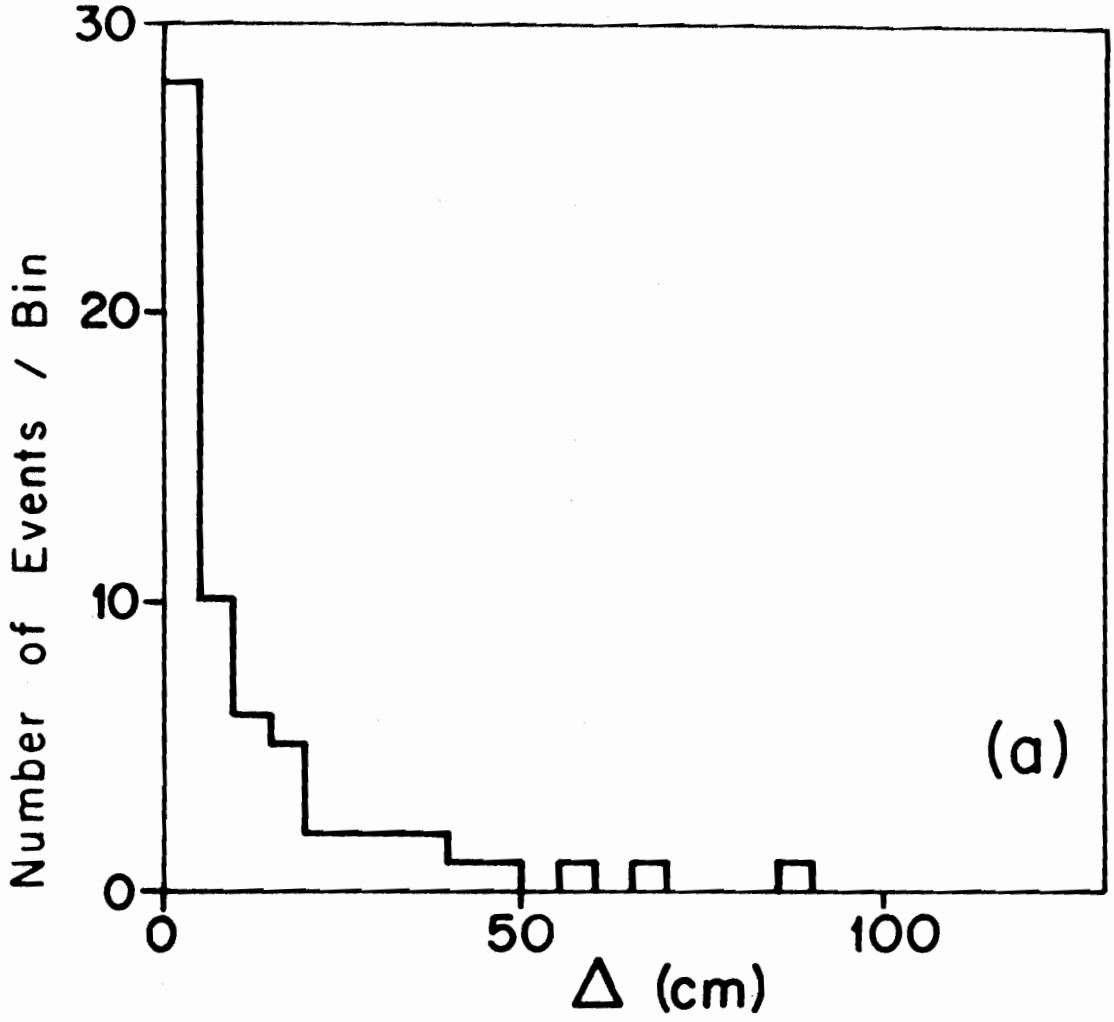
30
20
10
0
Number of Events / Bin
0
50
100
Δ (cm)
(a)

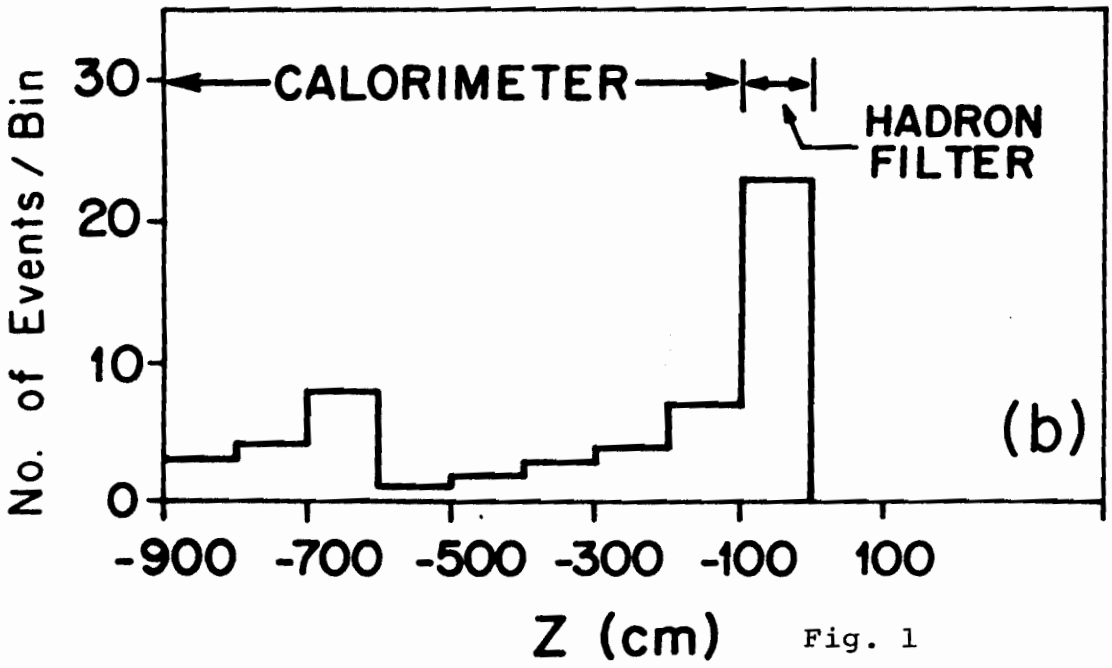
30
20
10
0
No. of Events / Bin
CALORIMETER
HADRON
FILTER
-900
-700
-500
-300
-100
100
Z (cm)
(b)

Fig. 1

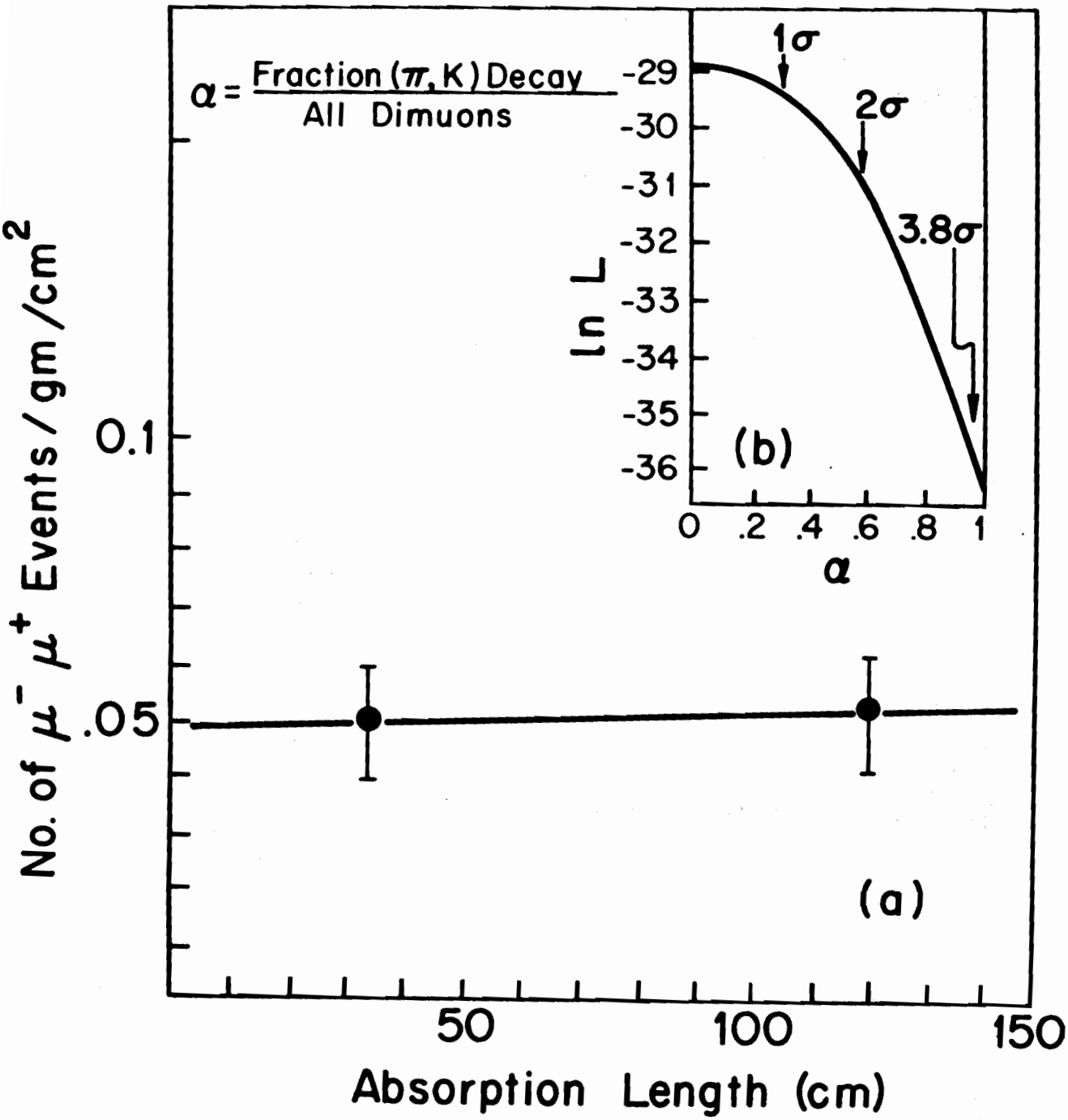
α = Fraction (π, K) Decay / All Dimuons
1σ
2σ
3.8σ
-29
-30
-31
-32
-33
-34
-35
-36
ln L
(b)
0
.2
.4
.6
.8
1
α
No. of μ⁻ μ⁺ Events / gm / cm²
0.1
.05
(a)
50
100
150
Absorption Length (cm)

Fig. 2

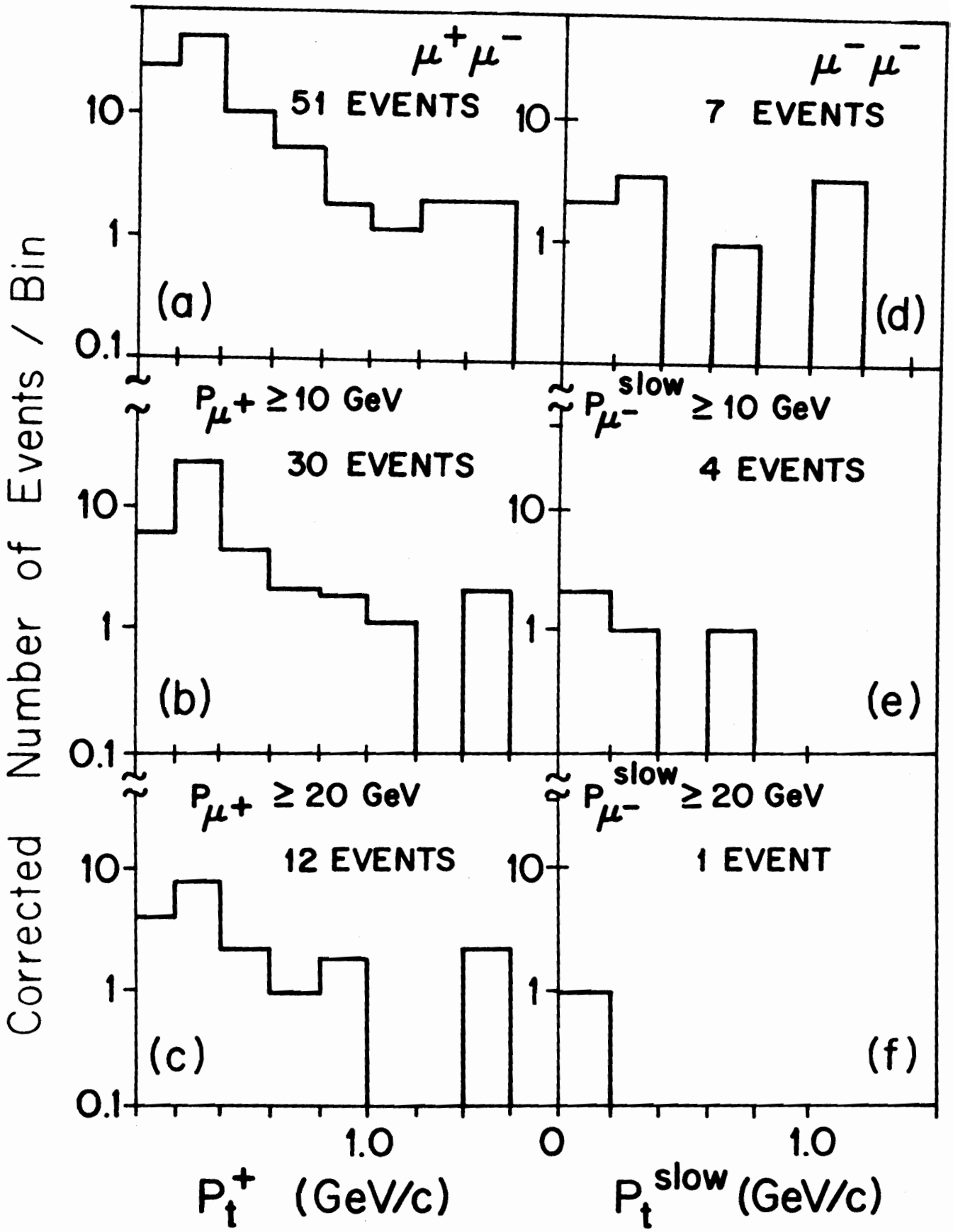
$\mu^+\mu^-$
51 EVENTS
(a)
$P_{\mu^+} \geq 10$ GeV
30 EVENTS
(b)
$P_{\mu^+} \geq 20$ GeV
12 EVENTS
(c)
$\mu^-\mu^-$
7 EVENTS
(d)
$P_{\mu^-}^{slow} \geq 10$ GeV
4 EVENTS
(e)
$P_{\mu^-}^{slow} \geq 20$ GeV
1 EVENT
(f)
Corrected Number of Events / Bin
10
1
0.1
1.0
0
P_t^+ (GeV/c)
P_t^{slow} (GeV/c)

Fig. 3

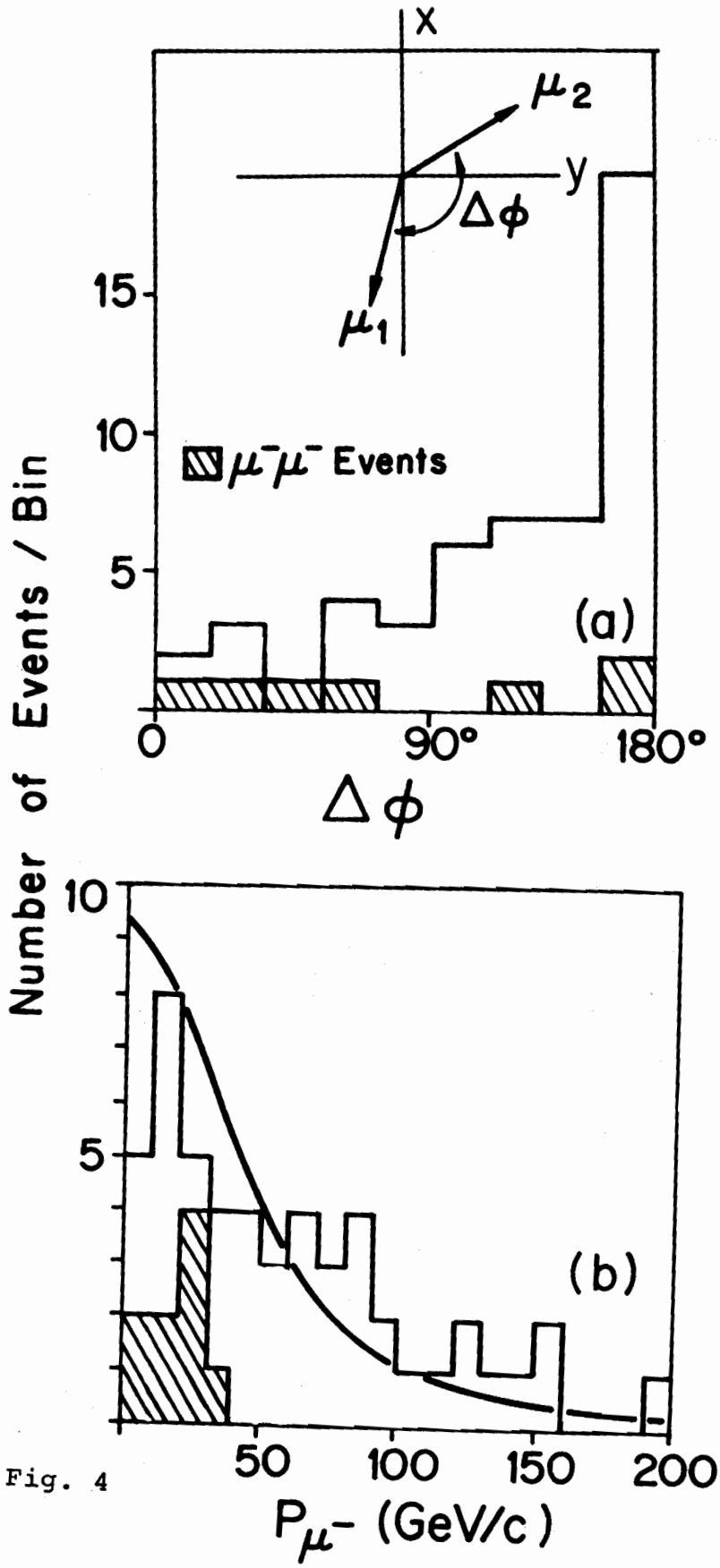
X
μ_2
y
$\Delta\phi$
μ_1
15
10
5
$\mu^-\mu^-$ Events
(a)
0
90°
180°
$\Delta\phi$
Number of Events / Bin
10
5
(b)
50
100
150
200
P_{μ^-} (GeV/c)

Fig. 4